International Journal of Science and Research (IJSR)
ISSN: 2319-7064
Impact Factor 2025: 7.089

# Advanced Simulation of Small-Arms-Class Ballistic Impact on Layered UHPC-FRC Protective Panels Using ANSYS Explicit Dynamics

**Harshal Kulthiya[1], Shreyanki Rai[2], Somaya Gangotiya[3], Kishor Patil[4]**

**Abstract:** ***This study presents a comparative numerical framework for evaluating the ballistic response of layered ultra-high-performance concrete (UHPC) and fiber-reinforced concrete (FRC) protective panels under small-arms class impact loading using ANSYS Explicit Dynamics. The Riedel-Hiermaier-Thoma (RHT) constitutive model was employed to capture strain-rate sensitivity, pressure-dependent strength, and progressive damage evolution in cementitious materials. Three target configurations with identical total thickness (100 mm) were investigated: a layered UHPC-FRC panel, a monolithic UHPC panel, and a monolithic normal-strength concrete (NSC) panel. Simulations were performed for projectile velocities ranging from 700 to 900 m/s using a rigid Truncated-Conical steel penetrator. Comparative performance was assessed through penetration depth, rear-face deformation, normalized penetration ratio, and energy-based response metrics. The UHPC and layered configurations showed stable penetration depths of approximately 60 mm across the investigated velocity range, while NSC exhibited substantially deeper penetration up to 91 mm. Rear-face deformation in the layered panel remained significantly lower than in NSC, indicating improved damage confinement and structural integrity. Although all configurations dissipated more than 99.93% of the projectile kinetic energy, the results demonstrate that ballistic performance depends primarily on energy redistribution and damage localization rather than total kinetic energy loss alone. The study provides a reproducible computational framework for comparative assessment of layered concrete protective systems under high-strain-rate impact conditions.***

**Keywords:** Ballistic impact; UHPC; FRC; layered concrete; explicit dynamics; RHT model; penetration resistance; energy dissipation; ballistic resistance; high-strain-rate behavior

## 1. Introduction

Protective elements built from concrete are a long-standing choice for defense installations and other critical infrastructure that must withstand high-velocity projectile impact. When subjected to ballistic loading, ordinary normal-strength concrete (NSC) generally fails in a brittle manner: the projectile opens a deep penetration channel, induces widespread internal cracking, and ejects material from the rear face (scabbing) [1,2].

Higher performance cementitious materials, notably ultra-high performance concrete (UHPC) and fiber-reinforced concrete (FRC), reach substantially higher compressive and tensile strengths than NSC and absorb significantly more impact energy [3,4]. Using either material on its own, however, does not fully exploit their complementary mechanical advantages under transient dynamic loading.

A layered architecture, in which a stiff UHPC layer is paired with a more ductile FRC layer, offers a natural way to combine these complementary advantages in a single protective element. Despite this potential, systematic numerical investigations that place such layered systems alongside their monolithic counterparts under a consistent modeling framework remain comparatively scarce [5,6].

The present work develops an explicit dynamic simulation framework to compare the ballistic response of layered UHPC-FRC panels against that of monolithic UHPC and NSC panels of identical total thickness, using a common set of energy based and deformation-based response metrics.

Existing studies often address either UHPC or RC behavior in isolation, or rely on differing constitutive frameworks, projectile geometries, and boundary conditions, which limits direct comparability of penetration resistance trends [3,4,5]. The novelty of the present study lies in the comparative explicit dynamics assessment of layered UHPC-FRC, monolithic UHPC, and NSC panels under identical small-arms class impact conditions using a consistent RHT based framework.

The contribution of the present study is not the generation of additional parametric trends or absolute prediction, but the mechanistic and comparative interpretation of energy redistribution and damage localization in layered concrete panels under identical impact conditions.

## 2. Numerical Methodology

### 2.1 Geometry and Configuration

The panel dimensions are 300 × 300 × 100 mm.
Configurations considered:

- Layered panel: 40 mm UHPC + 60 mm FRC
- Monolithic UHPC panel (100 mm)
- Monolithic NSC panel (100 mm)

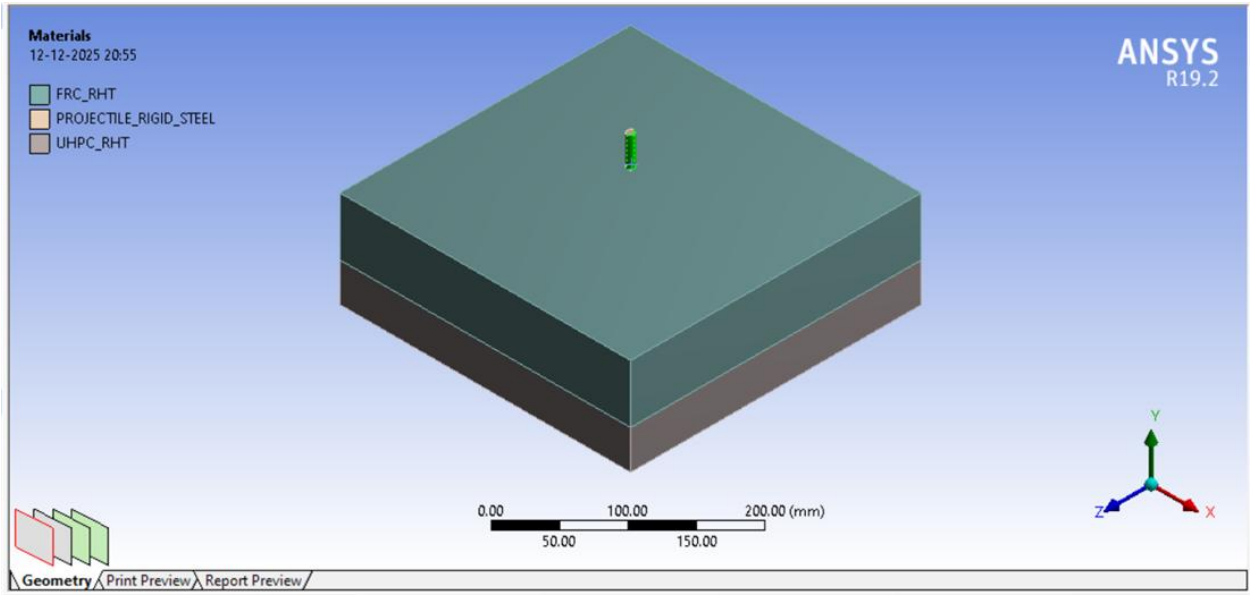


**Figure 1:** Geometry and configuration of the layered UHPC-FRC panel (300 × 300 × 100 mm) and projectile impact setup showing layer arrangement and impact direction

The 40 mm UHPC + 60 mm FRC layer ratio was selected to combine the high compressive strength of UHPC at the rear of the panel with the higher ductility and energy absorbing behaviour of FRC at the projectile strike face; this configuration aligns with the ductile front / strong backing concept commonly adopted in layered protective designs, and provides a controlled comparison baseline against the monolithic UHPC and NSC configurations of identical total thickness.

Figure 1. Geometry and configuration of the layered UHPC-FRC panel (300 × 300 × 100 mm) and projectile impact setup showing layer arrangement and impact direction

### 2.2 Projectile Description

A rigid steel projectile with truncated-conical nose geometry was adopted as a consistent surrogate penetrator across all simulations with the following characteristics:

- Density: 7850 kg/m³
- Geometry: cylindrical body with Truncated-Conical (frustum) nose
- Representative of small-arms class penetrator
- The projectile had a mass of 12.4 g

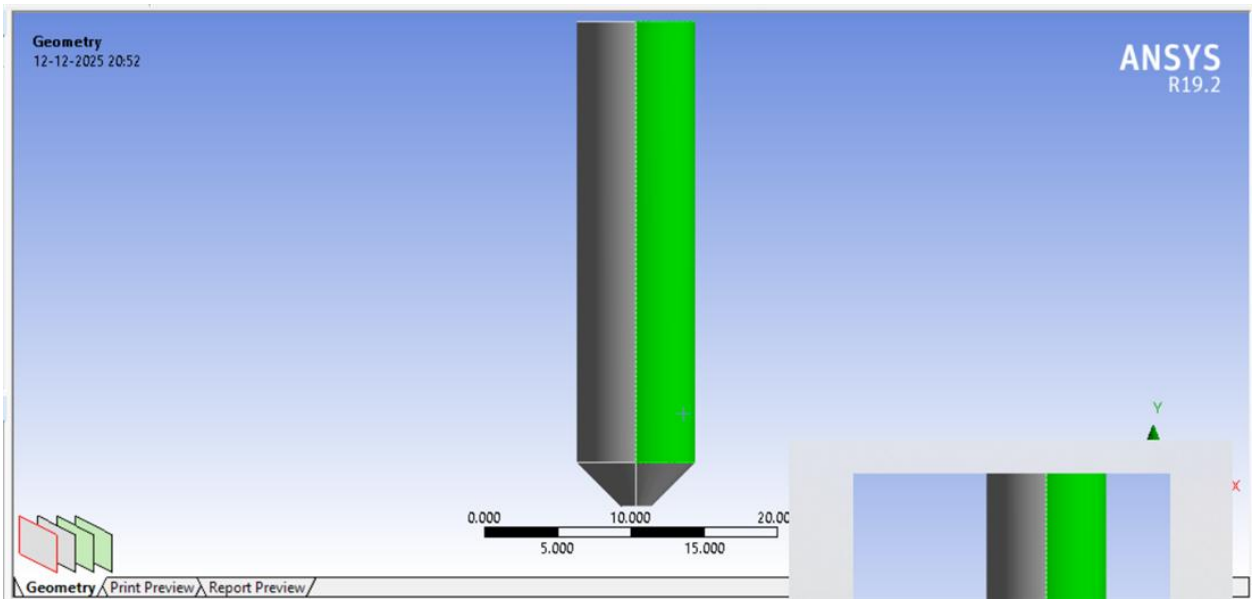


**Figure 2:** Geometry of rigid steel projectile with cylindrical body and truncated-conical nose used in the simulation

### 2.3 Material Modeling

All three concrete materials in this study (UHPC, FRC and NSC) are described using the Riedel-Hiermaier-Thoma (RHT) constitutive model. The RHT formulation accounts for the following features that are central to high-strain-rate concrete response:

- Pressure-dependent strength
- Strain-rate sensitivity
- Damage evolution and softening

The adopted parameters represent effective continuum properties for the investigated concrete classes and were not tuned to reproduce a specific experiment. RHT is selected for its ability to capture pressure-dependent brittle failure and strain-rate effects, and its suitability for concrete impact and ballistic problems has been demonstrated in prior verification, validation, and code comparison studies of RHT and related concrete impact models [7,8,11], including parameter modification studies that document RHT sensitivity to compressive strength variations and provide guidance for parameter selection [12].

Although case specific calibration was not performed, the adopted parameter sets were selected to remain within published ranges corresponding to the respective concrete classes, and the study is therefore interpreted comparatively rather than as an absolute predictive calibration. The complete RHT parameter set used for FRC, UHPC, and NSC, together with the elastic properties of the rigid steel projectile, is summarized in Table A1 (Appendix A).

### 2.4 Contact and Boundary Conditions

Projectile target interaction is modeled using frictionless surface to surface contact ($\mu = 0$), allowing separation after impact.
The projectile is modeled as a rigid body to isolate target response and eliminate projectile deformation effects.

Boundary conditions:
- Simply supported (SS)
- Fixed (reference cases)

Impact is normal to the panel surface with velocities ranging from 700 m/s to 900 m/s. Comparative conclusions are based primarily on simply supported cases.

### 2.5 Mesh and Numerical Stability

A graded mesh was adopted: a refined 1.5 mm element size on the impact zone Front-face, 2 mm on the rear-face region of the UHPC layer, and 5 mm in the bulk of the panel away from the impact zone, with the same mesh strategy maintained across all cases to preserve comparative integrity. No mass scaling is applied.

Mesh density is selected to ensure qualitative convergence of response trends; formal mesh convergence is not claimed, and the same impact zone refinement is applied across all cases so that relative comparisons remain valid even in the absence of an exhaustive sensitivity sweep.

Element erosion was not enabled; damage is represented using a continuous damage formulation.

Simulations were conducted for 0.001 s using a full three-dimensional explicit Lagrangian formulation.

### 2.6 Performance Metrics

The following metrics are evaluated:
- Penetration depth (P)
- Rear-face deformation ($\delta$)
- Normalized penetration (P/t)
- Normalized deformation ($\delta$/t)
- Projectile kinetic energy loss

Residual projectile velocity values are extracted from maximum nodal velocity of the rigid projectile and are used as comparative indicators rather than center of mass ballistic residual velocity.

## 3. Results and Discussion

### 3.1 Numerical Stability and Energy Balance

The simulations exhibit stable energy behavior, with smooth transfer of projectile kinetic energy into internal energy and plastic work. Total energy stability was preserved throughout each simulation (a drift below 1% of the initial system energy across all eight runs), and the hourglass control was set to the standard Explicit Dynamics value; no anomalous energy generation or hourglass energy dominance was observed, confirming numerical stability of the explicit dynamic solution.

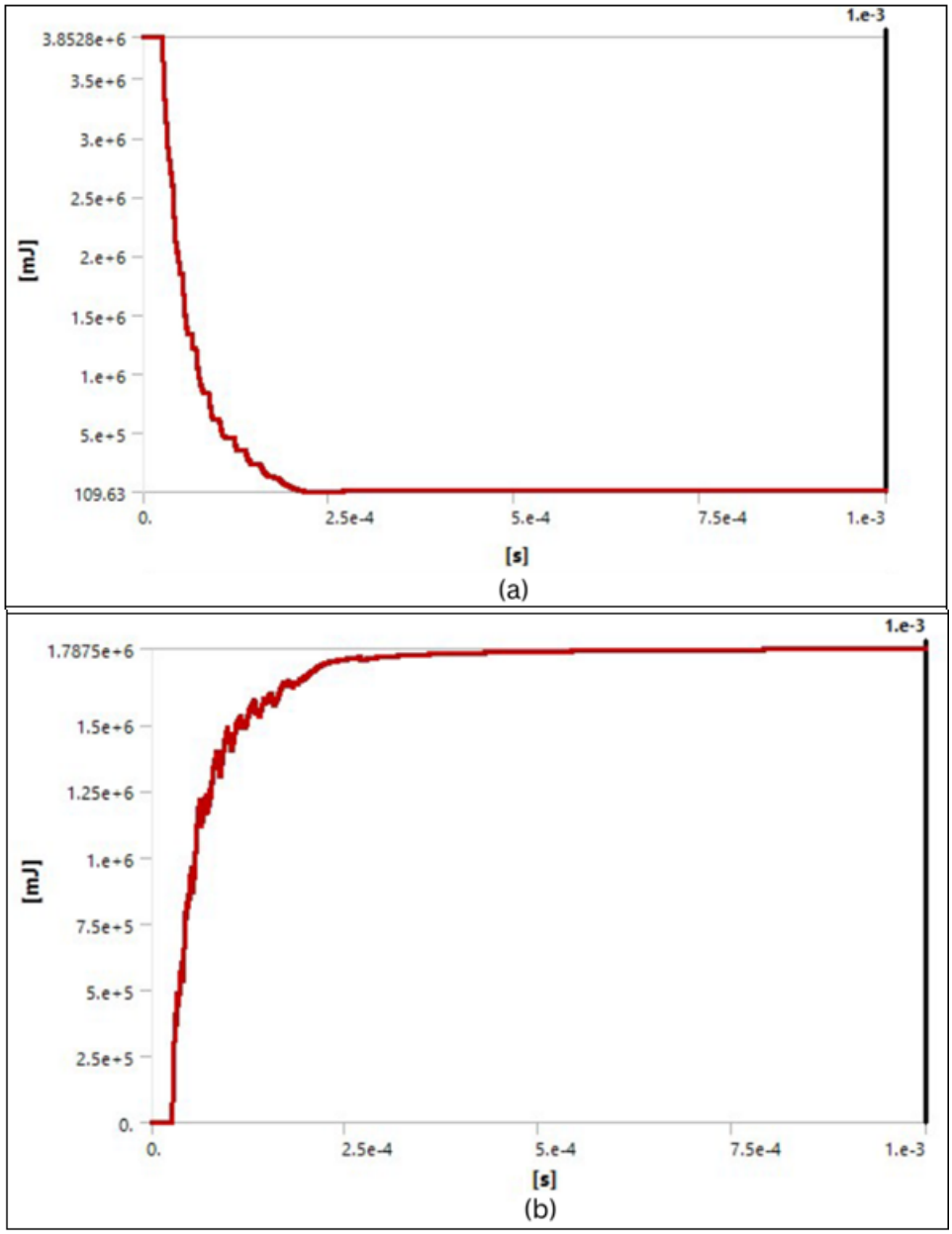


**Figure 3:** Energy evolution of the hybrid UHPC-FRC panel at 850 m/s: (a) projectile kinetic energy-time history and (b) model internal energy-time history

The internal energy represents the primary contribution to energy dissipation; however, additional components such as contact and numerical energies contribute to the total energy balance, which remains conserved throughout the simulation.

### 3.2 Penetration Behavior

Penetration depth exhibits limited sensitivity to impact velocity within the investigated 700 900 m/s regime, stabilizing at approximately 60 mm for both UHPC and layered panels, indicating a transition to layer controlled resistance once the projectile reaches the higher strength layer.

**Table 1:** Penetration comparison at 850 m/s

| Panel Type | Penetration (mm) |
|---|---|
| Hybrid (UHPC-FRC) | 60 |
| UHPC | 60 |
| NSC | 91 |

The results indicate that high strength materials govern penetration resistance, while NSC shows significantly deeper penetration. Within the investigated velocity range, the results suggest that penetration is governed more strongly by target resistance characteristics than on further increases in projectile velocity, consistent with the reduced sensitivity of penetration depth to compressive strength variations discussed in published UHPC ballistic reviews [3].

### 3.3 Damage and Failure Mechanism

The simulated damage fields differ markedly between the three panel configurations.

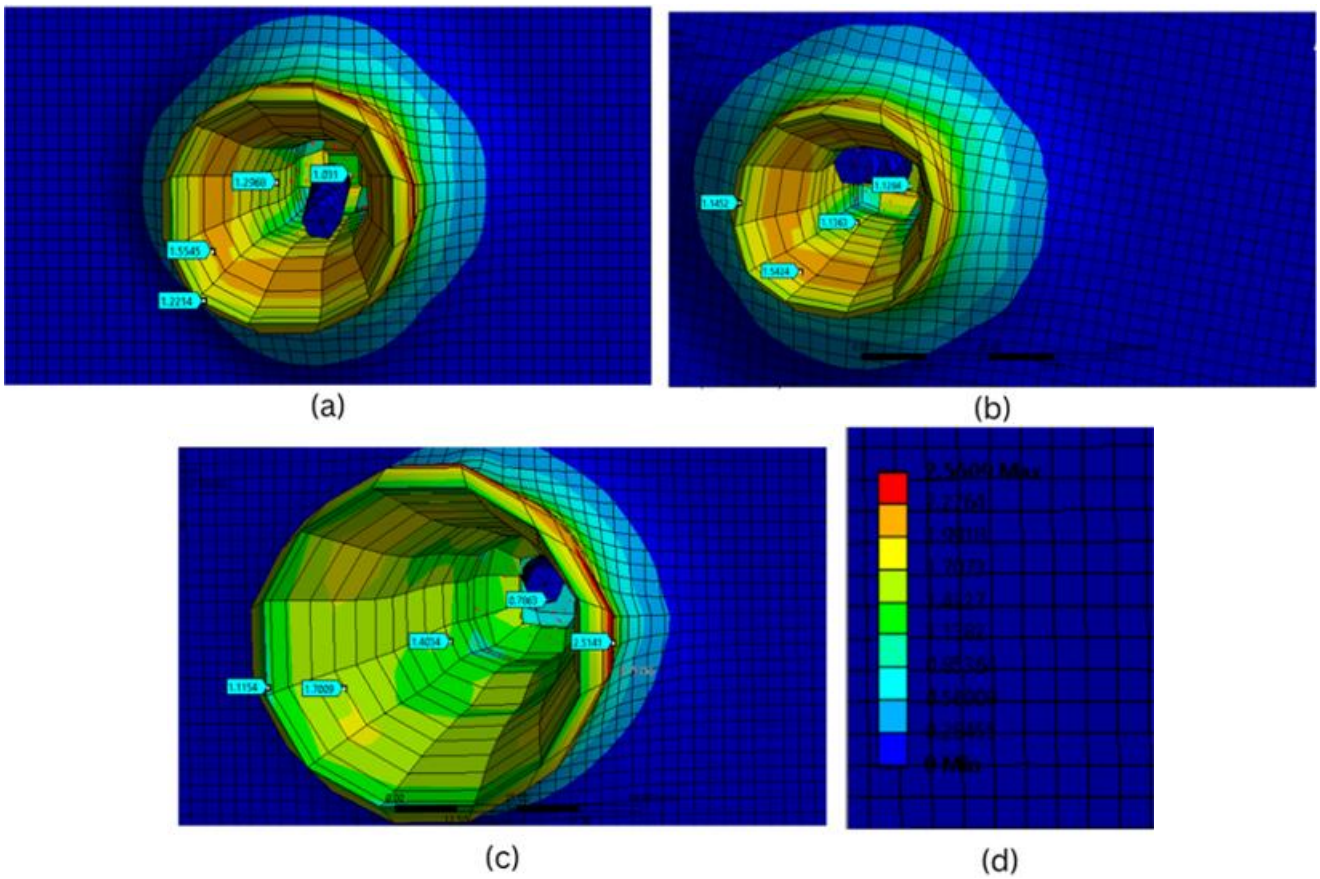


**Figure 4:** Equivalent plastic strain contours at peak response for (a) Hybrid (UHPC-FRC), (b) UHPC, and (c) NSC, with a common scale (d) at 850 m/s

The hybrid (UHPC-FRC) panel exhibits localized damage, whereas NSC shows widespread cracking and scabbing, in line with the brittle perforation and scabbing behavior reported for reinforced and plain concrete panels under high-velocity impact [4,2]. The improved damage confinement in UHPC and UHPC-FRC layers is consistent with the role of high strength matrices and fiber reinforcement in restricting crack growth and arresting fragment ejection [5,6,10]. The UHPC panel exhibits similarly confined damage with reduced rear-face disturbance, whereas the NSC panel shows a wider damage cone and greater strain localization depth.

### 3.4 Rear-face deformation

**Table 2:** Rear-face deformation comparison at 850 m/s

| Panel Type | Rear Deformation (mm) |
|---|---|
| Hybrid | 12-13 |
| UHPC | ~10 |
| NSC | 28 |

Reduced deformation in hybrid (UHPC-FRC) panels indicates improved energy confinement, consistent with the lower rear-face response reported for UHPC-based composite structures relative to conventional concrete [5].

### 3.5 Velocity Behavior

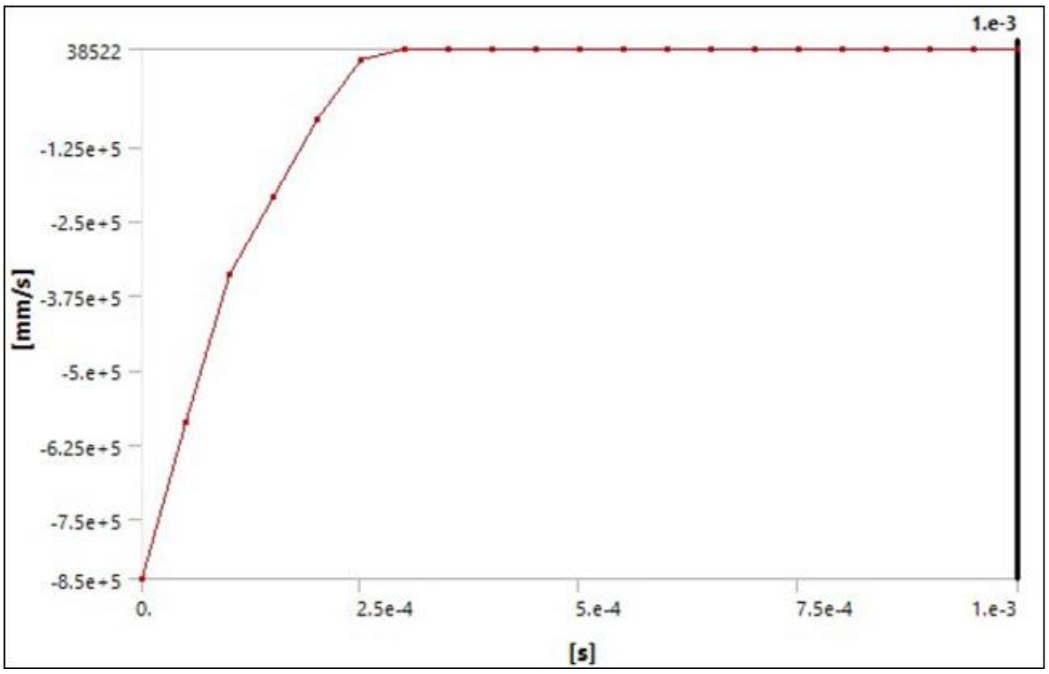


**Figure 5:** Projectile velocity time response showing rapid deceleration after impact on Hybrid (UHPC-FRC) Panel at 850 m/s

The projectile velocity time history shows rapid deceleration immediately after impact, followed by stabilization at a low residual nodal velocity level. These values represent extracted maximum nodal velocity of the rigid projectile and are used for comparative response assessment rather than center of mass residual velocity. The NSC residual velocity (20.19 m/s) being lower than that of the hybrid panel (38.52 m/s) at the same impact velocity does not imply superior NSC performance: the NSC panel achieves this velocity reduction through extensive penetration (91 mm) and large rear-face deformation (28 mm) i.e., by structural failure whereas the hybrid panel limits penetration to 60 mm and rear-face deformation to 12 13 mm. Residual velocity alone is therefore not a sufficient ballistic performance metric for this comparison.

### 3.6 Energy Dissipation

More than 99.93% of the initial projectile kinetic energy is lost across all configurations.

Taken together, these findings indicate that the ballistic ranking among the three panels is not determined by the overall magnitude of projectile kinetic energy loss, but by how efficiently that energy is redistributed inside the target through localized and controlled failure mechanisms.

Residual projectile kinetic energy remains below 3 J in all cases, indicating near complete energy transfer to the target. The higher energy redistribution efficiency of UHPC and UHPC-FRC layers, relative to NSC, is consistent with the enhanced post-cracking toughness and fiber-bridging mechanisms reported for fiber reinforced ultra-high performance concretes [6,3].

### 3.7 Normalized Performance

**Table 3:** Normalized performance parameters

| Panel | P/t | δ/t |
|---|---|---|
| Hybrid | 0.6 | 0.12 |
| UHPC | 0.6 | 0.1 |
| NSC | 0.91 | 0.28 |

To provide a consolidated comparison of energy related response metrics at 850 m/s, the key results are summarized in Table 4.

**Table 4:** Comparative Ballistic Performance at 850 m/s

| Panel Type | Residual Velocity (m/s) | Initial KE (J) | Final KE (J) | Projectile KE Loss (J) | Projectile KE Loss (%) |
|---|---|---|---|---|---|
| Hybrid (UHPC-FRC) | 38.52 | 4479.5 | 0.11 | 4479.4 | 99.9976 |
| UHPC | 14.87 | 4479.5 | 0.23 | 4479.3 | 99.995 |
| NSC | 20.19 | 4479.5 | 2.88 | 4476.6 | 99.9357 |

### 3.8 Benchmark Comparison with Literature

**Table 5:** Benchmark comparison of ballistic performance with literature

| Study | Thickness | Energy | P/t | Outcome |
|---|---|---|---|---|
| Kristoffersen et al. | 50 mm | 1.4-2.2 kJ | — | Ballistic limit |
| Present Hybrid | 100 mm | ~4.5 kJ | 0.6 | No perforation |
| NSC (present) | 100 mm | ~4.5 kJ | 0.91 | Near perforation |

Compared with the thin slab perforation study of Kristoffersen et al. [1], which reports a ballistic limit transition for 50 mm concrete slabs in the 1.4 2.2 kJ range, the present 100 mm hybrid (UHPC-FRC) panel exhibits a non-perforating response at an impact energy of approximately 4.5 kJ. Reinforced and ultra-high performance concrete panels in other ballistic studies have similarly shown reduced penetration depth and rear-face damage when high strength matrices and fiber reinforcement are present [4,5,6,9]. Direct quantitative comparison nonetheless remains limited by differences in projectile geometry and mass, slab thickness and aspect ratio, material grade and mix design,

boundary conditions, and modeling assumptions; therefore, the agreement reported here is interpreted as qualitative trend consistency rather than one to one experimental validation.

### 3.9 Comparative Literature Review

To contextualize the present comparative study against published ballistic impact and constitutive model work on concrete, Table 6 summarizes the priority literature with respect to test methodology, projectile and target configuration, impact velocity / energy range, constitutive model, and key reported outcomes. The selection covers experimental, numerical, and hybrid studies, three constitutive models (HJC, modified HJC, RHT), and impact regimes ranging from sub 200 m/s laboratory gas gun testing to 800 m/s real firearm tests on UHPFRC. Direct one to one quantitative comparison across these studies is inherently limited because no two share identical projectile geometry and mass, target dimensions and aspect ratio, material grade, mesh strategy, boundary conditions, or constitutive parameter set; Table 6 is therefore intended as a qualitative trend reference, and the present study is positioned in the final row using its own simulation derived metrics.

**Table 6:** Comparative summary of priority ballistic impact and constitutive model studies

| | Authors (Year) | Approach | Target | Projectile / Loading | Velocity / Energy | Model | Key Outcome |
|---|---|---|---|---|---|---|---|
| [1] | Kristoffersen et al. 2021 | Exp + Num (gas gun) | 50 mm plain concrete; C35/C75/C110 | 20 mm ogive-nose steel, 196 g | v_bl 118 152 m/s | MHJC (LS DYNA) | f_t dominates; 3x f_c gives ~20% v_bl gain |
| [2] | Kristoffersen et al. 2021 (conf.) | Exp + Num (air gun) | as [1] | as [1] | as [1] | MHJC | DYMAT/EPJ version of [1] |
| [3] | Das & Nanthagopalan 2022 | Review | UHPC literature | SHPB / blast / ballistic | Multiple regimes | | SOTA review of UHPC ballistic/blast |
| [4] | Dara & Alagappan 2024 | Num (LS DYNA) | RC 1 m x 1 m | Hemispherical, multi-impact | ~162 m/s | RHT class | Multi-impact > single in damage |
| [5] | Ning et al. 2023 | Exp + Num | UHPC Phi1300 x 600 mm | 30 mm steel, ~1 kg | 200 350 m/s | ANSYS/LS DYNA | UHPC: smaller crater than granite |
| [6] | Dapper et al. 2021 | Exp | UHPC 30/50/70 mm, hybrid fibers | Military | > 4000 J | | 3.0% hybrid fibers optimal |
| [7] | Grunwald et al. 2017 | Num V&V | Various (incl. C70/85) | Various | Wide range | RHT LS DYNA vs AUTODYN | LSD RHT matches AUTODYN |
| [8] | Heckotter & Sievers 2017 | Num model comp. | RC slabs (VTT/IRIS) | Hard missile | Various | RHT LSD vs AUTODYN | Tension regime differences; no fracture energy |
| [9] | Mina et al. 2021 | Exp (real-firearm) | UHPFRC 200 x 200 mm, 15 70 mm | 7.62 mm G3 rifle bullet | ~800 m/s | | 3+3% steel fiber mix best; only 15 mm perforated |
| [10] | Subair et al. 2023 | Review | UHPC fiber literature | | | | Review of fiber type/content/length |
| [11] | Bisht et al. 2022 | Num model assess. | Thin UHPC (H/d >= 5) | Per literature | Per literature | HJC (ABAQUS) | HJC suitable for thin UHPC |
| Present | | Num comparative | 300x300x100 mm; Hybrid/UHPC/NSC | 12.4 g truncated conic steel | 700 900 m/s (~3 5 kJ) | RHT (ANSYS Explicit) | Penetration 60 mm (Hybrid/UHPC) vs 91 mm (NSC); >99.93% KE loss |

**Table 7:** Quantitative ballistic impact comparison

| Ref | Study (year) | Panel material | Thickness (mm) | Projectile (mass) | V (m/s) | KE (kJ) | Penetration / Outcome | Comparative note |
|---|---|---|---|---|---|---|---|---|
| [1] | Kristoffersen 2021 | Plain C35 (f_c = 44.6 MPa) | 50 | Ogive-nose steel, 196 g | 119.7 (v_bl) | 1.40 | Perforation at v_bl | Same projectile mass class as present; ~3x lower KE; thin slab regime |
| [1] | Kristoffersen 2021 | Plain C75 (f_c = 72.8 MPa) | 50 | Ogive-nose steel, 196 g | 140.4 (v_bl) | 1.93 | Perforation at v_bl | 3x f_c gives only ~17% v_bl gain |
| [1] | Kristoffersen 2021 | Plain C110 (f_c = 112.5 MPa) | 50 | Ogive-nose steel, 196 g | 152.6 (v_bl) | 2.28 | Perforation at v_bl | High-strength concrete; brittle fragmentation |
| [5] | Ning 2023 | UHPC (f_c = 160 MPa) | 600 | 35CrMnSiA steel, 1001 g | 216 | 23.4 | DOP = 145 mm (no perforation) | Very thick UHPC block; ~80x heavier projectile than present |
| [5] | Ning 2023 | UHPC (f_c = 160 MPa) | 600 | 35CrMnSiA steel, 1003 g | 341 | 58.3 | DOP = 223 mm (no perforation) | h/d = 7.43; deep penetration regime, not directly comparable |
| [6] | Dapper 2021 | UHPC + 3.0% steel/PP hybrid fibers | 70 | Military projectile, n/r | n/r | up to 7.42 | No perforation (NIJ class III) | Similar thickness regime; fiber-bridging dominates |
| [9] | Mina 2021 | UHPFRC (3+3% hybrid steel fibers) | 15 | 7.62 mm G3 bullet, ~9.5 g | 800 muzzle / | 3.04 muzzle / | Perforated | Below the no perforation threshold for this UHPFRC mix |

| | | | | | | | | |
|---|---|---|---|---|---|---|---|---|
| | | | | | 726 at slab | 2.50 at slab | | |
| [9] | Mina 2021 | UHPFRC (3+3% hybrid steel fibers) | 30, 50, 70 | 7.62 mm G3 bullet, ~9.5 g | 800 muzzle / 726 at slab | 3.04 muzzle / 2.50 at slab | No perforation | Most directly comparable: real 7.62 mm small-arms field test |
| Present | This study (2026) | Hybrid UHPC-FRC (40 mm UHPC + 60 mm FRC) | 100 | Truncated conic steel, 12.4 g | 850 | 4.48 | DOP = 60 mm; no perforation | P/t = 0.60; layer-controlled saturation |
| Present | This study (2026) | Monolithic UHPC | 100 | Truncated conic steel, 12.4 g | 850 | 4.48 | DOP = 60 mm; no perforation | Matches hybrid in penetration; lower rear face deflection |
| Present | This study (2026) | Monolithic NSC (homogenized, unreinforced) | 100 | Truncated conic steel, 12.4 g | 850 | 4.48 | DOP = 91 mm; near perforation | P/t = 0.91; brittle scabbing |
| Trend | This study vs literature | Layered UHPC-FRC at 100 mm, 4.5 kJ | | | | | Non perforating | Consistent with [6] (UHPC + hybrid fibers >4 kJ) and [9] (UHPFRC 30+ mm at 3 kJ); penetration ranking NSC > UHPC = Hybrid is consistent with [1] (f_c effect) and [5] (UHPC reduces DOP vs lower strength matrices) |

of selected priority studies with the present work (values verified from source documents; n/r = not reported in source).

To complement the qualitative summary in Table 6, Table 7 reports a focused quantitative comparison between the present study and the literature cases for which projectile mass, impact velocity, panel thickness, and penetration outcome are explicitly available. Direct numerical comparison must again be treated cautiously because no two studies share identical projectile geometry, mass, target geometry, support conditions, or constitutive parameter set; for example, [5] uses a ~1 kg projectile against a 600 mm UHPC block, while [9] uses a real 7.62 mm bullet against 15 70 mm UHPFRC plates. The present work occupies an intermediate regime small-arms class energy (~3 5 kJ), moderate panel thickness (100 mm), and a comparative architecture in which the layered UHPC-FRC system shows a non-perforating response while NSC at the same projectile and velocity exhibits near perforation. This relative ranking is consistent with the trend observed in the cited literature.

## 4. Conclusions

The present study developed a comparative explicit-dynamics framework for evaluating layered UHPC-FRC, monolithic UHPC, and NSC protective panels under small-arms-class projectile impact. The numerical results demonstrated that the layered UHPC-FRC configuration achieved penetration resistance comparable to monolithic UHPC while significantly reducing rear-face deformation relative to NSC. Both UHPC-based systems exhibited stable penetration behavior across the investigated velocity range, whereas NSC showed substantially deeper penetration and greater damage spread. Although all targets dissipated nearly the entire projectile kinetic energy, ballistic performance was found to depend primarily on controlled energy redistribution and localized damage evolution rather than kinetic-energy loss alone. The study confirms the effectiveness of layered UHPC-FRC architectures for impact-resistant protective applications and provides a reproducible RHT-based computational framework for future simulation-driven design and optimization studies.

1) Layered UHPC-FRC panels exhibit stable penetration depth (~60 mm) across all impact velocities
2) Hybrid configuration matches UHPC in penetration resistance
3) Rear-face deformation is significantly reduced compared to NSC
4) More than 99.93% of the initial projectile kinetic energy is lost across all configurations.
5) Ballistic response is governed by how impact energy is redistributed and localized within the target.
6) Layered design improves impact resistance through controlled damage localization
7) The results indicate that effective ballistic performance in layered concrete systems is governed primarily by controlled energy redistribution and localized damage evolution rather than projectile kinetic energy loss alone.

## 5. Limitations

1) No experimental validation
2) Frictionless contact assumption ($\mu = 0$)
3) Rigid projectile modeling
4) Material parameters were adopted from validated literature sources without case specific calibration, which may influence absolute quantitative accuracy.
5) Single impact loading condition
6) Simulations are deterministic; variability is not considered.

Future work should extend the present framework to (i) deformable projectiles representative of real small-arms ammunition, (ii) multi-hit and obliquity scenarios on the same panel, (iii) experimental validation against gas gun and field firearm tests, and (iv) optimization of layer thickness ratios for specific threat classes. From an applied standpoint, the comparative ranking demonstrated here is directly relevant to defense infrastructure applications sentry posts, bunker walls, security barriers, and modular precast protective panels

where small-arms threats dominate the operational spectrum and where a layered UHPC-FRC architecture offers a path toward weight efficient passive protection. The reproducible RHT-based comparative framework reported in this study can therefore serve as a methodological stepping stone toward simulation led design of layered concrete protective elements for civil defense and military infrastructure.

**Data Availability**

The simulation input files, processed result tables, and post processing data used in this study are available from the corresponding author upon reasonable request. Public deposition was not undertaken because the working project files require software specific environments and institutional storage control.

**CRediT Author Statement**

Harshal Kulthiya (Corresponding Author): Conceptualization, Methodology, Software, Formal analysis, Writing original draft.
Shreyanki Rai: Software, Validation, Visualization.
Somaya Gangotiya: Supervision, Review & editing.
Kishor Patil: Review & editing.

**Declaration of Competing Interest**

The authors declare that they have no known competing financial interests or personal relationships that could have appeared to influence the work reported in this paper.

**Funding Sources**

This research did not receive any specific grant from funding agencies in the public, commercial, or not for profit sectors.

**Declaration of generative AI and AI assisted technologies in the manuscript preparation process**

During the preparation of this work, the authors used ChatGPT (OpenAI) for language refinement and structuring of the manuscript. After using this tool, the authors reviewed and edited the content as needed and take full responsibility for the content of the published article.

## References

[1] M. Kristoffersen, O. L. Toreskas, S. Dey, and T. Borvik, "Ballistic perforation resistance of thin concrete slabs impacted by ogive nose steel projectiles," Int. J. Impact Eng., vol. 156, art. no. 103957, Oct. 2021, doi: 10.1016/j.ijimpeng.2021.103957.

[2] M. Kristoffersen, O. L. Toreskas, S. Dey, and T. Borvik, "Ballistic impact on concrete slabs: An experimental and numerical study," EPJ Web Conf., vol. 250, art. no. 02001, 2021. [DYMAT 2021]

[3] N. Das and P. Nanthagopalan, "State-of-the-art review on ultra-high-performance concrete Ballistic and blast perspective," Cement Concrete Compos., vol. 127, art. no. 104383, Mar. 2022, doi: 10.1016/j.cemconcomp.2021.104383.

[4] R. U. N. Dara and P. Alagappan, "Ballistic impact response of reinforced concrete panels subjected to diverse multiple projectile impact scenarios: A numerical study," Indian Institute of Technology Madras, India. DOI: 10.1016/j.engfailanal.2024.108697

[5] H. Ning, H. Ren, W. Wang, and X. Nie, "Impact resistance of ultra-high performance concrete composite structures," Materials, vol. 16, no. 23, art. no. 7456, Nov. 2023, doi: 10.3390/ma16237456.

[6] P. R. Dapper, H. Z. Ehrendring, F. Pacheco, R. Christ, G. C. Menegussi, M. F. de Oliveira, and B. F. Tutikian, "Ballistic impact resistance of UHPC plates made with hybrid fibers and low-binder content," Sustainability, vol. 13, no. 23, art. no. 13410, Dec. 2021, doi: 10.3390/su132313410.

[7] C. Grunwald, B. Schaufelberger, A. Stolz, W. Riedel, and T. Borrvall, "A general concrete model in hydrocodes: Verification and validation of the RHT model in LS DYNA," Int. J. Prot. Struct., vol. 8, no. 1, pp. 58 85, Mar. 2017, doi: 10.1177/2041419617695977.

[8] C. Heckotter and J. Sievers, "Comparison of the RHT concrete material model in LS DYNA and ANSYS AUTODYN," Gesellschaft fur Anlagen und Reaktorsicherheit (GRS) gGmbH, Cologne, Germany, conference paper, 2017

[9] A. L. Mina, M. F. Petrou, and K. G. Trezos, "Resistance of an optimized ultra-high performance fiber-reinforced concrete to projectile impact," Buildings, vol. 11, no. 2, art. no. 63, Feb. 2021, doi: 10.3390/buildings11020063.

[10] S. Subair, A. Paul, and E. John, "The effect of fiber in ultra-high performance concrete (UHPC): A review," Int. J. Res. Eng. Sci. (IJRES), vol. 11, no. 6, pp. 141 151, Jun. 2023.

[11] M. Bisht, M. A. Iqbal, K. Kamran, V. Bratov, and N. F. Morozov, "Numerical study of thin UHPC targets response against ballistic impact," Mater. Phys. Mech., vol. 50, no. 1, pp. 74 88, 2022, doi: 10.18149/MPM.5012022_6.

[12] M. Abdel Kader, "Modified settings of concrete parameters in RHT model for predicting the response of concrete panels to impact," Int. J. Impact Eng., vol. 132, art. no. 103312, Oct. 2019, doi: 10.1016/j.ijimpeng.2019.06.001.

**Appendix A. RHT Material Parameters**

Table A1 summarizes the RHT constitutive parameters and elastic properties used for the three concrete materials (FRC, UHPC, NSC) and the rigid steel projectile. The concrete parameter sets were adopted from values reported in published RHT studies of impact and ballistic problems and were not recalibrated to a specific experiment; the present study is therefore interpreted comparatively rather than as an absolute predictive calibration. Sources used to guide parameter selection include the RHT verification and code comparison studies cited in Section 2.3 ([7], [8], [11], [12]).

**Table A1:** RHT and elastic material parameters used in this study.

| Property | FRC | UHPC | NSC | Rigid Steel (projectile) |
|---|---|---|---|---|
| Density (kg/m^3) | 2400 | 2500 | 2300 | 7850 |
| Young's Modulus E (GPa) | 35 | 45 | 30 | 210 |
| Poisson's ratio nu | 0.18 | 0.18 | 0.18 | 0.28 |
| Bulk modulus K (GPa) | 18.229 | 23.438 | 15.625 | 159.090 |
| Shear modulus G (GPa) | 14.831 | 19.068 | 12.712 | 82.031 |
| Use cap on elastic surface | Yes | Yes | Yes | N/A (rigid) |
| Compressive strength f_c (MPa) | 80 | 150 | 40 | N/A |
| Tensile strength ratio f_t/f_c | 0.12 | 0.10 | 0.10 | N/A |
| Shear strength ratio f_s/f_c | 0.19 | 0.18 | 0.18 | N/A |
| Intact failure surface constant A | 1.6 | 1.6 | 1.6 | N/A |
| Intact failure surface exponent n | 0.61 | 0.61 | 0.61 | N/A |
| Tension compression meridian ratio Q2.0 | 0.70 | 0.71 | 0.68 | N/A |
| Brittle to ductile transition BQ | 0.0035 | 0.0040 | 0.0030 | N/A |
| Hardening slope | 2.4 | 3.0 | 1.8 | N/A |
| Elastic strength / f_t (MPa) | 9.5 | 15.0 | 4.0 | N/A |
| Elastic strength / f_c (MPa) | 80 | 150 | 40 | N/A |
| Fracture strength constant B | 1.0 | 1.0 | 1.0 | N/A |
| Fracture strength exponent m | 0.61 | 0.61 | 0.61 | N/A |
| Compressive strain-rate exponent alpha | 0.018 | 0.021 | 0.016 | N/A |
| Tensile strain-rate exponent delta | 0 | 0 | 0 | N/A |
| Maximum fracture strength ratio SFMAX | 2.0 | 2.5 | 1.6 | N/A |
| Damage constant D1 | 0.02 | 0.01 | 0.03 | N/A |
| Damage constant D2 | 1.10 | 1.20 | 1.00 | N/A |
| Minimum strain to failure | 0.003 | 0.004 | 0.002 | N/A |
| Residual shear modulus fraction | 0.10 | 0.10 | 0.10 | N/A |
| Notes | Effective FRC properties | Reactive powder UHPC | Plain, unreinforced (homogenized) | Treated as rigid body; no plasticity / erosion |